Composites Part C: Open Access 9 (2022) 100303

Contents lists available at ScienceDirect

Composites Part C: Open Access

journal homepage: www.elsevier.com/locate/composites-part-c-open-access

Multiscale embedded models to determine effective mechanical properties of composite materials: Asymptotic Homogenization Method combined to Finite Element Method

Bruno Guilherme Christoff [a,*], Humberto Brito-Santana [b], Ramesh Talreja [c], Volnei Tita [a,d]

[a] Department of Aeronautical Engineering, Sao Carlos School of Engineering, University of Sao Paulo, Sao Carlos, SP, Brazil
[b] Departamento de Matematica, Facultad de Ciencias Naturales, Matematica y del Medio Ambiente, Universidad Tecnologica Metropolitana, Santiago, Chile
[c] Department of Aerospace Engineering, Texas A&M University, College Station, TX, USA
[d] Department of Mechanical Engineering, Faculty of Engineering of the University of Porto, Porto, Portugal

ARTICLE INFO

Keywords:
Finite Element Method
Virtual tensile testing
Asymptotic Homogenization Method
Multiscale embedded models

ABSTRACT

A reliable way to determine the effective properties of heterogeneous media plays an important role in engineering design. As an experimental test to obtain effective properties may be tedious and expensive to perform, and as computational approaches, when all heterogeneities of the media are considered during the simulations, might become impractical due to computational effort, homogenization procedures are a good alternative to estimate the effective properties of the media, mainly considering damage and manufacturing defects in the material. Among several homogenization methods, the Asymptotic Homogenization Method (AHM), a well-established mathematically based method, is considered for deriving the relations for the effective properties of the media, and the Finite Element Method (FEM) is used to solve the equilibrium relations. In this work, a fiber-reinforced composite is considered, with three different regions depicted: intact, damaged fibers, and regions with resin/void pockets. The proposed AHM-FEM approach is used to simulate a tensile test in all scenarios with standard and multiscale embedded Unit Cells used to obtain the effective elastic modulus on the fiber direction. Discussions regarding computational efficiency are carried out, as well as numerical comparisons among the types of Unit Cells used to model the media. In a second scenario, the complete fourth-order elasticity tensor of the media is investigated, considering the fibers as both isotropic and transversely isotropic. The results for the transversely isotropic fibers approach literature data, while when isotropic fibers are considered, poor results are achieved. Finally, the approach is extrapolated to obtain the mechanical properties of metamaterials, defined here as a composite reinforced by two different kinds of fibers.

1. Introduction

The determination of the effective elastic properties of heterogeneous media plays an important role in engineering design. As the use of cellular and composite materials increases, the need for developing reliable tools to predict their behavior also increases. The correct prediction of the mechanical properties in heterogeneous media, such as composite and cellular materials, mainly with damage and manufacturing defects, may allow a lower cost, lighter and/or with a higher specific strength design.

The effective mechanical properties of heterogeneous media can be obtained based on both macroscopic and microscopic theories.

The macroscopic models do not explicitly take the base material properties into account and are often limited to in-plane properties. On the other hand, the microscopic models are based on homogenization theories [1], and aim to study the behavior of the heterogeneous media wherein the interaction of the constituent materials is examined on a microscopic scale to determine their effect on the properties of the heterogeneous media [2].

Among several homogenization methods found in literature, one can highlight the Asymptotic Homogenization Method (AHM), which is based on a mathematically rigorous theory and has been used in several applications in the past years. In this method, a periodic Unit Cell (UC) is used to depict the microstructure of the material and its effective properties are obtained through a variational formulation on a local boundary value problem [3].

The well established AHM was first introduced in the seventies and contributions to the early development of the method can be attributed to [4–6]. Further contributions made by [7–15] discuss mathematical

* Corresponding author.
E-mail address: brunochristoff@usp.br (B.G. Christoff).

https://doi.org/10.1016/j.jcomc.2022.100303
Received 20 June 2022; Accepted 30 July 2022
Available online 13 August 2022

aspects, engineering applications and the use of the finite element method to solve the homogenization relations.

In recent years, the AHM has been used to find the effective elastic constants for several engineering applications, by using both numerical and analytical analyses. An effort has also been made to obtain the analytical solutions of AHM for specific representative volume elements that represent a heterogeneous media.

In [16] a two-scale Asymptotic Homogenization Method is used to investigate failure envelopes of unidirectional fiber-reinforced composites. A methodology is proposed, in which, for given stress applied to the macro level, it is possible to obtain the stress field at the micro-level. Three regions are considered, fiber, matrix, and interface, each one ruled by its failure mechanism. Besides, the authors show that the methodology is capable of calculating numerical failure envelopes with good approximation to experimental data. A semi-analytical method is proposed by [17] to obtain the effective properties of fiber reinforced composites with transversely isotropic constituents, in which the AHM relations are solved by the finite element method, and the results compared to exact solutions.

In the work of [18], a numerical Asymptotic Homogenization Method is used to obtain effective elastic properties of unidirectional fiber-reinforced composites, in which square and perfect hexagonal unit cells are employed. The results are compared to experimental data with good agreement, and discrepancies found between numerical and experimental data are explained in terms of simplifications considered in the homogenization method.

The effective complex-value of a three-phase elastic fiber-reinforced composite with parallelogram unit cell is studied in [19,20]. The two-scale AHM is considered and close analytical expressions for the local problems and the out-of-plane shear homogenized coefficient are derived. The authors also study the shear effective properties enhancement for the three-phase fiber-phase fiber-reinforced composite.

In [21], a multiscale methodology is proposed to predict the effective coefficients for layered composites with delamination on the macro-scale considering the influence of debonding between fiber and matrix on the micro-scale. The micro-scale problem is solved by the Finite Element Method, whilst the macro-scale problem is solved by both the Finite Element Method and the Asymptotic Homogenization Method.

In a study by [22], the effective elastic properties of layered composites are obtained by considering the influence of non-imperfect adhesion between plies, or in practical terms, delamination between adjacent plies. The authors address the problem by using two- and three-layer composites. The analytical expressions based on AHM are derived and compared to the Finite Element Solution.

The effect of localized damage in the interface between two layers of a laminated composite on the effective properties is investigated by [21]. The effect of delamination extensions is studied by both analytical and numerical solutions of the AHM. Additionally, the authors extrapolate the numerical approach to simulate a specific case in which the interface is considered as a functionally graded material. In a subsequent work [23], the authors consider an unbalanced laminated composite and both analytical and numerical solutions are derived. An interphase degradation between plies is considered, and a great agreement between the effective mechanical properties obtained by analytical and numerical approaches is observed.

By using a three scales asymptotic homogenization approach, [24] studies the effective behavior of hierarchical linear elastic composites reinforced by aligned fibers, in which each hierarchical level of organization has a periodic structure. The results focus on the effective out-of-plane shear modulus and are compared to literature data. In a similar approach, [25] uses the three scales asymptotic homogenization to investigate the in-plane and out-of-plane effective properties of hierarchical linear elastic solids. [26] proposes a multiscale asymptotic expansion to derive analytically the effective coefficients for fibrous and wavy laminated composites, in which the local problem is based on the application of Muskhelishvili's complex potentials in the form of Taylor and Laurent series.

Additionally, the application of periodic boundary conditions is crucial in analyses involving the numerical determination of effective properties of heterogeneous media. In the work of [27], a consistent application of periodic boundary conditions in both implicit and explicit finite element analysis is proposed, in which the influence of the periodic boundary conditions in the mechanical response under tension is addressed. The authors also investigate the computational performance between implicit and explicit solutions.

Furthermore, some studies also compare the AHM to experimental results. In [28], it is shown the AHM asymptotically converge to the exact solution by sequentially solving problems at different scales of hierarchy. In the work of [29], it is shown that the effective properties of composites with a periodic structure, such as stiffness and local strain, are better approximated using the homogenization theory instead of other well-established homogenization methods. Different methods for calculating the effective elastic properties in composite materials are investigated in [30], and the authors show that the results obtained by AHM approach experimental data. A semi-analytical approach, combining the Finite Element Method and the Asymptotic Homogenization Method, is developed in [31] to obtain the effective properties of periodic elastic-reinforced nanocomposites. The effect of the geometrical shape of the inclusions, volume fraction and length on the effective elastic properties are addressed and the results show a good agreement with experimental values.

In addition, an effort has been made in recent years to implement the Asymptotic Homogenization method by using a commercial finite element package. This kind of approach is appealing since commercial software may provide a wide finite element and material libraries, as well as pre-and post-processing tools. In [32], a complete implementation methodology for AHM in Abaqus^{TM} is presented. The authors show that the proposed methodology is capable of providing good results for the micro-mechanical analysis of stress in fiber-reinforced composites for unit cells with different fiber arrangements. In the work of [33] the authors present a complete methodology to implement the AHM in a form of a user-friendly plug-in, using Abaqus^{TM}. The potentialities of the method are explored by using several materials and elements provided by Abaqus^{TM} and the validation of the methodology is made by comparing the results obtained with the plug-in to analytical results found in the literature. [34] presents a simple implementation method for the AHM developed with a commercial Finite Element software as a toolbox. A set of simple boundary conditions are assumed and the effective elastic constant of the media is found after static analyses. Examples are performed and validated by comparing them with other methods.

In summary, the AHM is a mathematically rigorous method that presents accurate results when compared to experimental data and is still widely used to tackle problems involving the mechanical properties of heterogeneous media. Moreover, some recent work focuses on the implementation of AHM on commercial finite element software, providing a powerful tool to find the effective fourth-order elasticity tensor of heterogeneous materials. However, the use of AHM implemented in a commercial finite element software, its potentialities, and its numerical aspects, are yet to be investigated.

Thus, the numerical aspects of AHM, and the potentialities of using the method within a commercial finite element package, are addressed in the present work, which is rarely seen in the literature, and it is named as AHM-FEM approach.

Considering the aforementioned aspects, this work has as a main objective the determination of the effective properties of a fiber laminated composite, or a virtual tensile test, by using the proposed AHM-FEM approach. It is also intended to verify the influence of the Unit Cell on the effective properties of the media. Thus, several Unit Cells are used and compared for both intact and damaged materials. Here, the

benefits of using multiscale embedded models for the damaged models are shown.

The last objective is to compare the effective properties obtained by the AHM, considering the fiber as a transversely isotropic material, to literature results. In addition, the procedure is extrapolated and used to obtain the effective properties of metamaterials, in which a composite comprised of two different kinds of fibers is considered.

Hence, we initially present the approach used to tackle the problem. Intact and damaged portions of a fiber-reinforced composite are modeled using standard, and multiscale embedded Unit Cells. The mathematical background of the Asymptotic Homogenization Method is briefly presented, as well as the numerical solution via finite element analyses.

The results are presented in two sections. The first one investigates the effective elastic modulus in the fiber direction and the second one investigates the complete fourth-order elasticity tensor of the media. In addition, the approach is extrapolated to assess the effective properties of a metamaterial comprised by a composite reinforced by two different types of fibers.

The complete homogenization procedure is performed in a user-friendly software implemented by the authors alongside the finite element package Abaqus™ in a previous work [33].

2. Approach

Let Ω be a domain in $\mathbb{R}^3$ with boundary $\partial\Omega$, representing a unidirectional fiber-reinforced composite, as shown in Fig. 1.

Consider that the Dirichlet and Neumann boundary conditions are applied on $\partial\Omega_u$ and $\partial\Omega_f$, respectively, where

$$\partial\Omega = \partial\Omega_{u_i} \cup \partial\Omega_{f_i}; \quad \partial\Omega_{u_i} \cap \partial\Omega_{f_i} = \emptyset \quad i = 1,2,3, \tag{1}$$

such that

$$u_i = u_i^g \quad on \quad \partial\Omega_{u_i} \quad i = 1,2,3, \tag{2}$$

where u_i is the ith component of the displacement and u_i^g is known, and

$$\sigma_{ij} n_j = t_i \quad on \quad \partial\Omega_{t_i} \quad i = 1,2,3 \tag{3}$$

where $\boldsymbol{\sigma}$ is the stress tensor, $\boldsymbol{n}$ is a normal vector and t_i is the traction. Two coordinate systems are used in the definition of the problem. The macroscopic level, in which the effective properties of the media are considered, is defined by $\boldsymbol{x}$, and the microscopic level, in which a Unit Cell (UC) of the media is depicted, is defined by $\boldsymbol{y}$. Both coordinate systems are considered to be coincident.

In Fig. 1, distinct areas within the domain are highlighted representing three different regions of the unidirectional fiber-reinforced composite. The first region represents an intact material, whilst the second one considers a region in which the fibers are damaged, and the third one considers a region containing resin, or void, pockets within the composite.

Two main scenarios are considered to represent the three regions in the domain. In the first scenario, a small portion of the domain is represented by a standard Unit Cell containing only the fibers and the matrix. The second scenario considers a multiscale embedded Unit Cell comprised of fibers, matrix, and a surrounding embedded region formed by a homogenized material representing the composite.

The first part of the analysis performed aims to simulate virtual tensile tests to obtain the effective elastic modulus in the fiber direction. Initially, the intact material is considered and the influence of the dimensions of the Unit Cell, as well as the number of fibers used to represent the media, and the distribution of the fibers on the effective properties of the media are considered. Here, the results are compared to literature results, including the results provided by a composite manufacturer. In addition, a convergence analysis is performed for each Unit Cell.

In the next analysis, a region with damaged fibers is considered. Here, we use both the regular, and the multiscale embedded Unit Cells. Several severity degrees of damage are considered and convergence analyses are performed for both cases. In the last analyses, an embedded Unit Cell is considered to determine the effective elastic modulus of the material, when a resin/void pocket is present. Several volume fractions of the pockets are considered as well as four different shapes for the pockets.

In the second part of the analysis, the complete fourth-order elasticity tensor of the media is obtained. The analyses are performed considering the mechanical properties of the fiber both isotropic and as transversely isotropic, and the effective properties are compared to literature data.

Finally, the approach is extended to obtain the elastic properties of metamaterials, considering a multiscale embedded UC. In this case, the outer portion of the is homogenized and comprised of the properties obtained by considering the transversely isotropic fibers. The inner portion is comprised of fiber and matrix. Two different fibers are considered and all independent effective properties of the media are obtained as a function of the volume fraction of the material added to the media.

For all analyses, the AHM-FEM approach is used, i.e., the Asymptotic Homogenization Method is considered for the determination of the effective properties of the media, and the relations are solved by the Finite Element Method. The derivation of the relations is presented in the next section.

3. Asymptotic homogenization method

The Asymptotic Homogenization Method (AHM) is used to obtain the effective properties of the media. The notation, the derivation of the equilibrium problems and the finite element solution are based on [23,33,35,36].

The Asymptotic Homogenization Method (AHM) uses the concept of a Unit Cell (UC) to describe a heterogeneous media, in other words, there is a small portion of the domain that repeats itself in a pattern describing the whole domain. Additionally, an anisotropic and periodic elastic body is considered and the problem is formulated in the bounded subset $\Omega^\varepsilon \in \mathbb{R}^3$ is considered.

The method follows, basically, three assumptions [37]. The first one considers that, for the elasticity problem, the displacement field of the media can be written as an asymptotic expansion, as

$$\boldsymbol{u}^\varepsilon(\boldsymbol{x}) = \boldsymbol{u}^{(0)}(\boldsymbol{x}) + \varepsilon \boldsymbol{u}^{(1)}(\boldsymbol{x},\boldsymbol{y}) + \varepsilon^2 \boldsymbol{u}^{(2)}(\boldsymbol{x},\boldsymbol{y}) + \cdots \tag{4}$$

where $\boldsymbol{x}$ and $\boldsymbol{y}$ are the coordinates in the macroscopic and the microscopic levels, respectively, $\boldsymbol{u}^\varepsilon$ is the total displacement field and $\boldsymbol{u}^{(0)}$, $\boldsymbol{u}^{(1)}$ and $\boldsymbol{u}^{(2)}$ are the contributions for the displacement field of the macroscopic scale, microscopic scale, and eventual smaller scales, respectively. Eq. (4) shows that the displacement field of the global problem is dependent on the fast variable $\boldsymbol{y}$, and that implies that the secondary variables, such as the stress field are also dependent on the fast variable.

The second consideration is related to the relation between the two domains used in the description of the problem and states that the analysis can be made by using two separate scales, one at the microscopic level (Unit Cell) and another one at the macroscopic level (heterogeneous media) and that both are related by a small parameter $\varepsilon \ll 1$, such as

$$\boldsymbol{y} = \frac{\boldsymbol{x}}{\varepsilon} \tag{5}$$

meaning that the local problem domain is considerably smaller than the global problem domain. Thus,

$$\boldsymbol{Y} = \{\boldsymbol{y} = (y_1, y_2, y_3) \in \mathbb{R}^3 : 0 < y_i < l_i, \quad i = 1,2,3\} \tag{6}$$

denotes the Unit Cell, with l_i as a positive number, and

$$\Omega^\varepsilon = \varepsilon Y = \{\boldsymbol{x} = (x_1, x_2, x_3) \in \mathbb{R}^3 : \varepsilon^{-1} x_i \in Y, \quad i = 1,2,3\}, \tag{7}$$

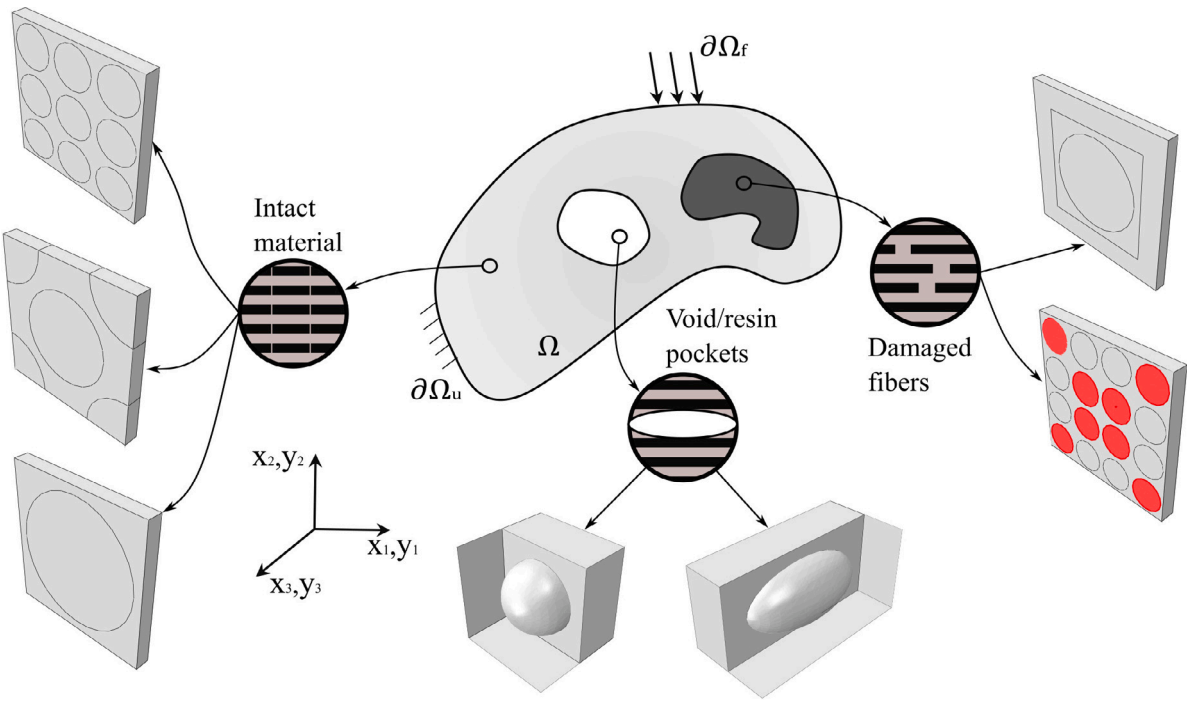

Fig. 1. Representation of the domain and the three distinct regions within the composite material: (i) Intact material and Unit Cells comprised of fiber and matrix; (ii) Material with damaged fibers - A UC comprised of damaged fibers, matrix, and an outer layer of homogenized material and a UC comprised with damaged fibers, intact fibers and matrix; (iii) Material containing void or resin pockets and UCs comprised by an outer portion of homogenized intact material and spherical or ellipsoidal inclusions representing the void or resin pockets (internal view).

alongside Eq. (5) denotes the global domain.

The third consideration is that the displacements on the boundaries of the Unit Cell are periodic. This consideration implies that the local domain itself is periodic, i.e., it repeats itself in a periodic pattern, thus describing the macroscopic domain.

A general field variable f_i^ϵ is thus dependent on both fast and slow variables, such as

$$f_i^\epsilon(\boldsymbol{x}) = f_i(\boldsymbol{x}, \boldsymbol{y}) \tag{8}$$

and its partial derivatives take the form

$$\frac{\partial f_i^\epsilon}{\partial x_j} = \frac{\partial f_i}{\partial x_j} + \epsilon^{-1}\frac{\partial f_i}{\partial y_j}. \tag{9}$$

Assuming no body forces acting on the media, one can write the elastic equilibrium as

$$\frac{\partial \sigma_{ij}^\epsilon}{\partial x_j} = 0 \quad \text{in} \quad \Omega^\epsilon, \tag{10}$$

where

$$\sigma_{ij}^\epsilon = C_{ijkl}(\boldsymbol{y})\frac{\partial u_k^\epsilon}{\partial x_l}. \tag{11}$$

Using the asymptotic expansion, Eq. (4), and the stress field, Eq. (11), yields

$$\sigma_{ij}^\epsilon(\boldsymbol{x}) = \sigma_{ij}^{(0)}(\boldsymbol{x}, \boldsymbol{y}) + \epsilon u_i^{(1)}(\boldsymbol{x}, \boldsymbol{y}) + \epsilon^2 u_i^{(2)}(\boldsymbol{x}, \boldsymbol{y}) + \cdots, \tag{12}$$

where

$$\sigma_{ij}^{(m)}(\boldsymbol{x}, \boldsymbol{y}) = C_{ijkl}(\boldsymbol{y})\frac{\partial u_k^{(m)}}{\partial x_l} + C_{ijkl}(\boldsymbol{y})\frac{\partial u_k^{(m+1)}}{\partial y_l}, \ldots, m = 0, 1, 2, \ldots \tag{13}$$

Now, using Eqs. (4) and (12) into Eq. (10), and rearranging and grouping like exponents ϵ, one has for ϵ^{-1} and ϵ^0, respectively

$$\frac{\partial \sigma_{ij}^{(0)}}{\partial y_j} = 0 \tag{14}$$

and

$$\frac{\partial \sigma_{ij}^{(0)}}{\partial x_j} + \frac{\partial \sigma_{ij}^{(1)}}{\partial y_j} = 0. \tag{15}$$

Using Eq. (13) for $m = 0$ and (14) one has

$$\frac{\partial}{\partial y_j}\left(C_{ijkl}\frac{\partial u_k^{(1)}}{\partial y_l}\right) = -\frac{\partial C_{ijkl}}{\partial y_j}\frac{\partial u_k^{(0)}}{\partial x_l} \tag{16}$$

where the solution is represented in the form

$$u_i^{(1)}(\boldsymbol{x}, \boldsymbol{y}) = \chi_i^{jk}(\boldsymbol{y})\frac{\partial u_j^{(0)}(\boldsymbol{x})}{\partial x_k} \tag{17}$$

and thus the following local problem is obtained:

$$\frac{\partial}{\partial y_j}\left(C_{ijkl}\frac{\partial \chi_k^{pq}}{\partial y_l} + C_{ijpq}\right) = 0 \quad \text{in} \quad Y, \tag{18}$$

with

$$\left[\chi_k^{pq}\right] = 0 \tag{19}$$

and

$$\left[C_{ijkl}\frac{\partial \chi_k^{pq}}{\partial y_l} + C_{ijpq}\right] n_j = 0 \quad \text{on} \quad \Gamma, \tag{20}$$

where Γ is the interface in the unit cell Y.

Note that Eqs. (18) and (20) can also be obtained from the equilibrium state given by

$$\int_Y C_{ijpq}\frac{\partial \chi_p^{kl}}{\partial y_q}\frac{\partial v_i}{\partial y_j}\,dY = -\int_Y C_{ijkl}\frac{\partial v_i}{\partial y_j}\,dY, \tag{21}$$

where $\boldsymbol{v}$ is a virtual displacement field.

Assuming $m = 0$ in Eq. (13), and considering Eq. (17), one obtains

$$\sigma_{ij}^{(0)} = \left(C_{ijpq} + C_{ijkl}\frac{\partial \chi_k^{pq}}{\partial y_l}\right)\frac{\partial u_p^{(0)}}{\partial x_q}. \tag{22}$$

The macroscopic equilibrium is obtained by the averaging Eq. (15) as

$$\frac{\partial \left\langle \sigma_{ij}^{(0)} \right\rangle_Y}{\partial x_j} = 0 \tag{23}$$

where

$$\left\langle \sigma_{ij}^{(0)} \right\rangle_Y = \frac{1}{|Y|} \int_Y \sigma_{ij}^{(0)} dY = C_{ijkl}^H \frac{\partial u_k^{(0)}}{\partial x_l} \tag{24}$$

with

$$C_{ijkl}^H = \left\langle C_{ijkl} + C_{ijhs} \frac{\partial \chi_h^{kl}}{\partial y_s} \right\rangle_Y, \tag{25}$$

which is the homogenized fourth-order elasticity tensor of the media. The cell average operator is defined as

$$\langle \bullet \rangle_Y = \frac{1}{|Y|} \int_Y \bullet \, dY. \tag{26}$$

In summary, the general elasticity problem of finding the effective fourth-order elasticity tensor consists in solving the equilibrium problem, finding χ, such that

$$\int_Y C_{ijpq} \frac{\partial \chi_p^{kl}}{\partial y_q} \frac{\partial v_i}{\partial y_j} dY = -\int_Y C_{ijkl} \frac{\partial v_i}{\partial y_j} dY \tag{27}$$

that can be used to find the effective properties of the media by using

$$C_{ijkl}^H = \frac{1}{|Y|} \int_Y \left(C_{ijkl} + C_{ijpq} \frac{\partial \chi_p^{kl}}{\partial y_q} \right) dY. \tag{28}$$

The characteristic displacement field, χ^{kl}, is the periodic solution of Eq. (27) and it is used in Eq. (28) to find the elastic constants of the effective elastic tensor. For a general three-dimensional case, the indexes i, j, p, q, k and l assume values between 1 and 3, and the elastic tensor has 21 independent constants. To obtain all constants, it is sufficient to solve Eq. (27) for the load cases $kl = 11$, $kl = 22$, $kl = 33$, $kl = 12$, $kl = 23$ and $kl = 13$.

There are several ways to solve the integral equations of the homogenization method, and several authors derived the analytical relations for specific cases. However, the set of Eqs. (27) and (28) may be tedious to obtain analytically, mainly when complex geometries and materials are considered. Thus, the finite element method is employed to solve the equilibrium problem by the imposition of periodic displacements applied directly to the global arrays of the problem. The equilibrium problem, stated in Eq. (27), can be written in a vectorial form as [15, 38]

$$\int_Y \left(\frac{\partial \boldsymbol{v}}{\partial \boldsymbol{y}} \right)^T \boldsymbol{C} \frac{\partial \boldsymbol{\chi}}{\partial \boldsymbol{y}} \, dY = -\int_Y \left(\frac{\partial \boldsymbol{v}}{\partial \boldsymbol{y}} \right)^T \boldsymbol{C} \, dY \tag{29}$$

If the Unit Cell is divided into finite elements, the virtual displacements $\boldsymbol{v}$, and the characteristic solution $\boldsymbol{\chi}$ can be written, respectively, as [39]

$$\frac{\partial \boldsymbol{v}}{\partial \boldsymbol{y}} = \boldsymbol{B}\hat{\boldsymbol{v}} \tag{30}$$

and

$$\frac{\partial \boldsymbol{\chi}}{\partial \boldsymbol{y}} = \boldsymbol{B}\hat{\boldsymbol{\chi}} \tag{31}$$

where $\hat{\boldsymbol{v}}$, and $\hat{\boldsymbol{\chi}}$ are, respectively, the nodal virtual displacement vector and the nodal characteristic displacement vector, and $\boldsymbol{B}$ is the global strain–displacement matrix.

Eqs. (30) and (31) are now used in the equilibrium problem of Eq. (29), rendering

$$\int_Y (\boldsymbol{B}\hat{\boldsymbol{v}})^T \boldsymbol{C} \boldsymbol{B}\hat{\boldsymbol{\chi}} dY = -\int_Y (\boldsymbol{B}\hat{\boldsymbol{v}})^T \boldsymbol{C} dY. \tag{32}$$

Since the virtual displacements are arbitrary, they can be chosen in a such way that

$$\int_Y \boldsymbol{B}^T \boldsymbol{C} \boldsymbol{B}\hat{\boldsymbol{\chi}} dY = -\int_Y \boldsymbol{B}^T \boldsymbol{C} dY. \tag{33}$$

Eq. (33) resembles a standard finite element equilibrium, and it can be written as

$$\boldsymbol{K}\hat{\boldsymbol{\chi}} = -\boldsymbol{f} \tag{34}$$

where $\boldsymbol{K}$ is the UC stiffness matrix, and $\boldsymbol{f}$ is the homogenization load vector. This equation represents the global equilibrium of the UC when submitted to the homogenized load.

For a single element, e, of the mesh, the local stiffness matrix is given by

$$\boldsymbol{K}^e = \int_{Y^e} \boldsymbol{B}^{eT} \boldsymbol{C}^e \boldsymbol{B}^e dY^e, \tag{35}$$

and, by using a quadrature scheme to evaluate the integral, it can be written as

$$\boldsymbol{K}^e = \sum_{m=1}^{p} \left(\boldsymbol{B}_m^{eT} \boldsymbol{C} \boldsymbol{B}_m^e \right) W_m J_m, \tag{36}$$

where p is the number of quadrature points used in the integration, W_m and J_m are, respectively, the quadrature weight and the determinant of the Jacobian matrix, which is associated with the mth quadrature point. Similarly, the local homogenized load vector is given by

$$\boldsymbol{f}^e = \int_Y \boldsymbol{B}^{eT} \boldsymbol{C}^e dY, \tag{37}$$

and, using a quadrature scheme, it is written as

$$\boldsymbol{f}^e = \sum_{m=1}^{P} \left(\boldsymbol{B}_m^{eT} \boldsymbol{C}^e \right) W_m J_m. \tag{38}$$

The global arrays are assembled in the standard way. It is important to highlight that the characteristic displacement field $\boldsymbol{\chi}$ is periodic, thus, periodicity constraints have to be applied in the global arrays to enforce that consideration.

A similar procedure is used to discretize the integral equation (28), and it can be written as

$$\boldsymbol{C}^H = \frac{1}{|Y|} \int_Y (\boldsymbol{C} + \boldsymbol{C}\boldsymbol{B}\hat{\boldsymbol{\chi}}) \, dY. \tag{39}$$

The integral equation (39) can be substituted by a sum through all elements of the mesh and solved by a quadrature scheme, as

$$C_{ijkl}^H = \sum_{e=1}^{N_{EL}} \sum_{m=1}^{P} \left(C_{ijkl}^{(e)} + C_{ijrs}^{(e)} B_r^{(e)(m)} \hat{\chi}_s^{kl(e)} \right) W_m J_m, \tag{40}$$

where N_{EL} is the total number of elements on the mesh.

Thus, the equilibrium equation (34) is solved for six load cases (tractions in the 3 directions – y_1, y_2 and y_3; shear on the 3 planes – y_1y_2, y_1y_3 and y_2y_3) and used in Eq. (40) in order to obtain the homogenized fourth-order elasticity tensor of the media.

All the analyses are performed in a code implemented alongside the finite element package Abaqus™ by the authors in a previous work [33].

4. Virtual tensile test via the AHM-FEM approach

This section presents the results of the virtual tensile test performed by using the Asymptotic Homogenization Method solved by the Finite Element Method. The first objective is to obtain the effective elastic modulus in the fiber direction, by an analysis of the Unit Cell (UC) and compare it to literature data. An experimental tensile test [40] is considered as comparison base, in which an Hexcel® M10 pre-impregnated carbon reinforced composite is used.

In a second analysis, it is considered that a volume fraction of the fibers in the composite is damaged, and both a regular, and a multiscale embedded Unit Cell models are used to tackle the problem. The third analysis considers void and resin pockets in an embedded UC model.

The relevant data for the simulations are given in Table 1, and it is considered that the composite is reinforced by fibers aligned in x_3–direction. In addition, all the simulations are performed using

Table 1
Composite material data.

Description	Value	Reference
Fiber Young's modulus	231.0 GPa	[41]
Matrix Young's modulus	3.2 GPa	[40]
Fiber volume fraction	0.6	[42]

Table 2
Reference values for the effective Young's modulus.

Value	Nomenclature	Reference
127.0 GPa	Reference (i)	[40]
132.0 GPa	Reference (ii)	[43]
140.0 GPa	Reference (iii)	[42]
148.0 GPa	Reference (iv)	[44]

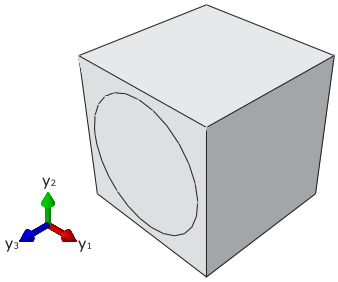

Fig. 2. Unit Cell used for the influence of the dimension of the domain. The cases considered are $L_1 = L_2 = L_3 = 1.0$. $L_1 = L_2 = L_3 = 2.0$ and $L_1 = L_2 = L_3 = 4.0$.

the user-friendly plug-in implemented by the authors in a previous work [33]. For all presented cases, the eight-node trilinear isoparametric with full integration (C3D8) is used and a convergence analysis is performed for every case.

4.1. Intact media and influence of the unit cell type

In the first case, we investigate the influence of the type of the UC on the effective elastic modulus in the fiber direction. It is considered that the media is intact and that there is a perfect bond between fiber and matrix. The objective is to vary the parameters used to describe the Unit Cell as a representation of the domain. Thus, we want to verify the robustness of the AHM-FEM approach, and find the most numerically efficient way of tackling the problem. The cases considered used different dimensions for the Unit Cells, distinct fiber distribution patterns, and also the number of fibers used to describe the domain.

All the results are compared to the literature data given in Table 2. In addition, a convergence analysis is performed for each case as a numerical efficiency factor.

The first analysis considers an UC with equal dimensions, as shown in Fig. 2. The influence of those dimensions are investigated and the cases $L_1 = L_2 = L_3 = 1.0$, $L_1 = L_2 = L_3 = 2.0$, and $L_1 = L_2 = L_3 = 4.0$ are considered. Fig. 3 shows the analyses of convergence, and the comparison with the literature results.

In this particular case, no significant difference is noticed. By analyzing Eq. (39), one can see that the properties are obtained by the average of the UC size. As proportional values are used in the simulation, the results themselves are also proportional.

The slight differences in the convergence of the UCs can be explained by the mesh generation procedure. Since no regular mesh is used, and an automatic mesh generation is adopted, the finite element mesh might vary from one case to another, rendering thus some numerical fluctuations in the final result.

The second considered case investigates the influence of the thickness in the fiber direction of the UC on the effective properties of the media. Fig. 4 shows the UC considering the dimensions in the fiber

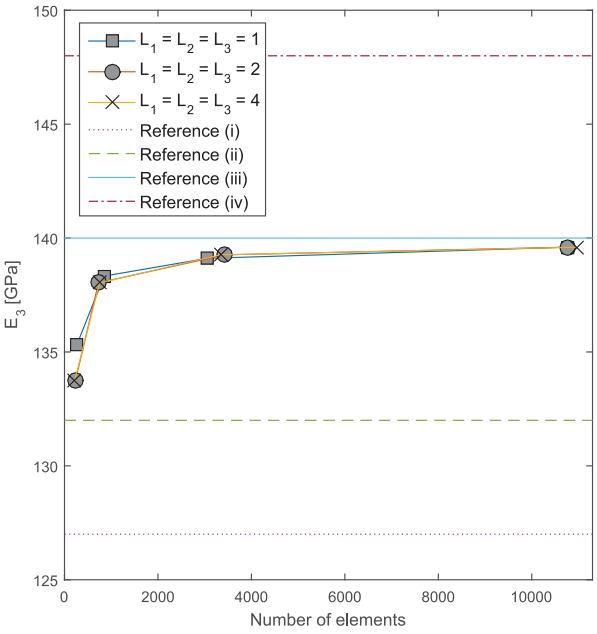

Fig. 3. Convergence analysis. Influence of the dimensions of the UC and comparison with the reference values.

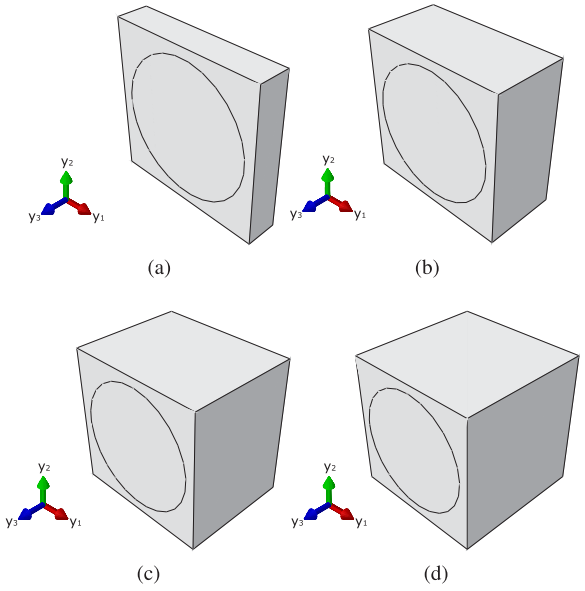

Fig. 4. Unit Cells used for the influence of the dimension in y_3 direction. (a) $L_3 = 0.2$, (b) $L_3 = 0.5$, (c) $L_3 = 0.8$, and (d) $L_3 = 1.0$.

direction as $L_3 = 0.2$, $L_3 = 0.3$, $L_z = 0.3$ and $L_3 = 1.0$. The dimensions $L_1 = 1.0$ and $L_2 = 1.0$ remain constant in all analyses.

Fig. 5 shows the convergence analyses for all considered cases and the comparison to literature data. In this case, it is noticed that, the shorter the dimension L_3, the better the mesh convergence. This result shows that for this particular case, we can model the UC so that the convergence of the result is enhanced.

Those analyses show that the AHM method can easily take advantage of the symmetries of the problem. Moreover, as periodicity constraints are used on the boundaries of the UC, all cases shown in Fig. 4 are representative of a fiber-reinforced composite. Besides, despite all cases converging to the same effective elastic modulus, the convergence rate increases with the reduction of the length in the fiber direction adopted in the analyses. Thus, this kind of analysis shows that

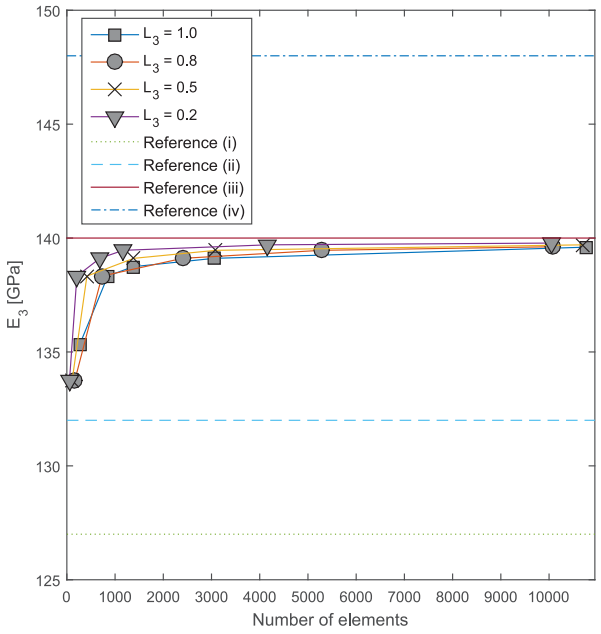

Fig. 5. Convergence analysis. Influence of the length in y_3 direction and comparison with the reference values.

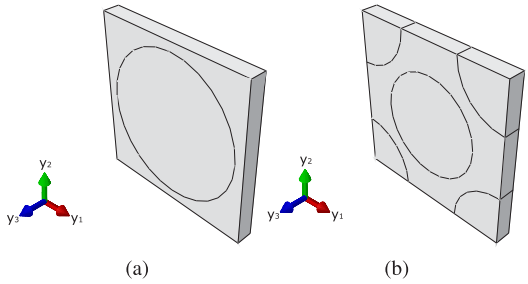

Fig. 6. Unit Cells used for the influence of the fiber distribution. (a) UC 1, and (b) UC 2.

the computational effort can be reduced depending on how the method is used.

In a subsequent analysis, two fiber distributions are considered, as shown in Fig. 6. The first Unit Cell (UC 1) is comprised of a single centralized fiber, whilst the second Unit Cell (UC 2) is comprised of a centralized fiber, and four-quarters of the fiber is on the edges. Both cases have the same fiber volume fraction.

The convergence analyses and the comparison to literature data are shown in Fig. 7. As one can notice, both Unit Cells converge to the same value for the effective elastic modulus, however, UC 1 has a better convergence rate than UC 2. Although both Unit Cells represent the same composite and have the same fiber volume fraction, UC 2 is more complex in terms of the geometry itself. Thus, more elements are needed to faithfully represent the geometry and, consequently, more elements are needed to achieve the convergence.

It is also important to highlight that, despite the effective elastic modulus on the fiber direction not being significantly affected by the fiber distribution in the domain, the mechanical properties of the directions perpendicular to the fiber do change with different fiber distributions. Thus, if other properties are considered, a more cautious procedure has to be employed. In other words, similar analyses should be performed if other properties were determined.

In a last analysis of the intact material, the influence of the number of fibers used to represent the UC is considered. Fig. 8 shows the Unit

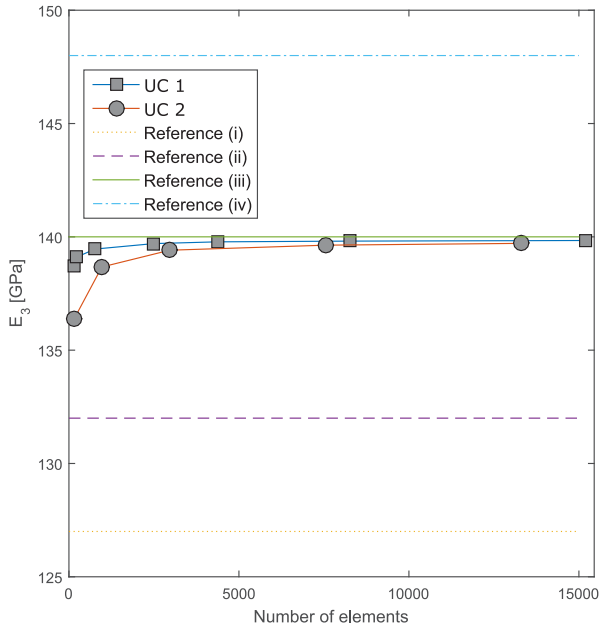

Fig. 7. Convergence analysis. Influence of the fiber distribution and comparison with the reference values.

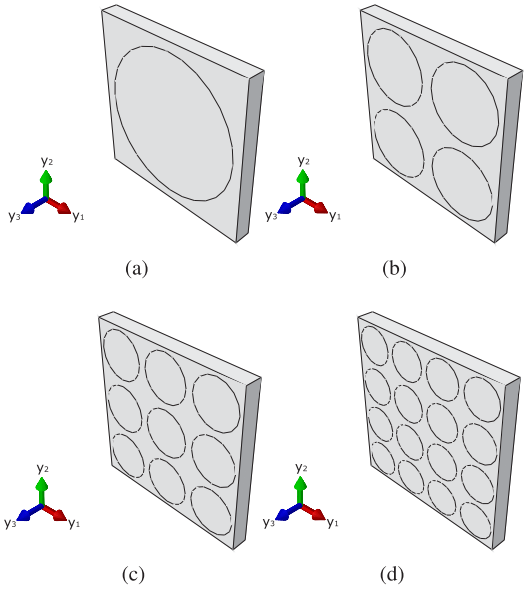

Fig. 8. Unit Cells used for the influence of the number of fibers. (a) 1 fiber, (b) 4 fibers, (c) 9 fibers, and (d) 16 fibers.

Cell representation for one, four, nine and sixteen regularly distributed fibers.

The convergence analyses for all cases and the comparison to the literature data are shown in Fig. 9. It is clear that the more fibers used in the representation of the UC, the poorer the convergence of the result. This can be explained by the same reasoning used before. First, the more fibers used, the more complex the geometry of the UC, and thus, more elements have been used to discretize the domain, which affects the convergence rate of the analysis. In addition, the single fiber UC takes advantage of the periodicity constraints of the problem using a less complex UC, enhancing the convergence rate significantly in comparison to the representations using more fibers.

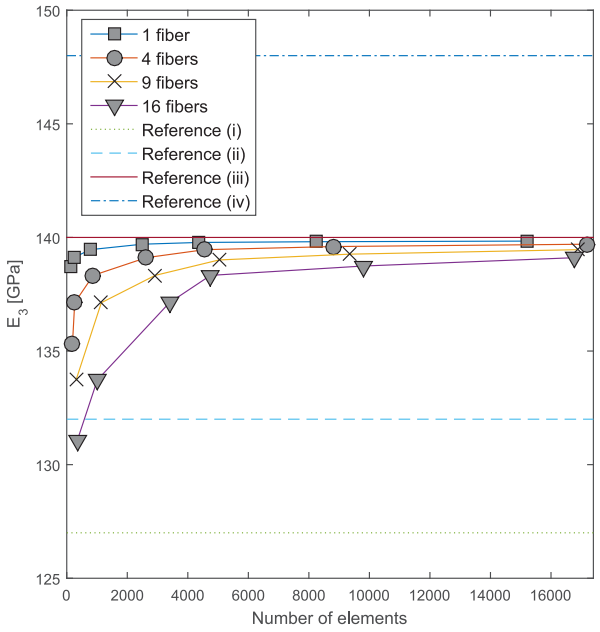

Fig. 9. Convergence analysis. Influence of the number of fibers and comparison with the reference values.

The analyses performed show that the Asymptotic Homogenization Method solved via the Finite Element Method is robust to obtaining the effective elastic modulus of a composite material. In all cases, the results converge to the elastic modulus provided by the manufacturer [42].

In addition, several aspects intrinsic to the AHM can be used to improve the computational efficiency of the analyses in terms of mesh convergence, such as the periodicity constraints and the complexity of the Unit Cell chosen to represent the domain.

4.2. Multiscale embedded models and influence of fiber failure

In this section, it is considered that a fraction of the fibers in the composite is damaged. In this case, a damage pattern is adopted, i.e., it is considered that a representative parcel of the domain has an amount, or volume fraction, of the fibers, damaged. With this consideration, two distinct Unit Cells are used to approach the analyses. The first one considers a regular UC, in which both damaged and intact fibers and the matrix are modeled. The second UC is represented by an embedded model described by a single damaged fiber, matrix, and an outer layer of homogenized material representing the intact parcel.

The damage pattern applied consists of degenerating the mechanical properties of the fibers. Thus, the damaged fibers are unable to add stiffness to the material. The properties of the damaged fibers are considered as 0.1% of the properties of the intact fibers, and the properties of the homogenized outer layer are the ones obtained in the previous section.

For the first comparison, the damaged fiber volume fractions considered are 25% and 50%. Fig. 10 (a) and (c) show the regular Unit Cells with 25% and 50% of fibers damaged and Figures (c) and (d) their embedded model counterparts.

Fig. 11(a) shows the convergence analysis for the UC models with 25% with fibers damaged and Fig. 11(b) the convergence analyses for the cases with 50%.

Both the multiscale embedded, and standard UC models converge to the same value for the effective elastic modulus, however, the convergence rate of the regular UC is slower than their multiscale embedded counterparts.

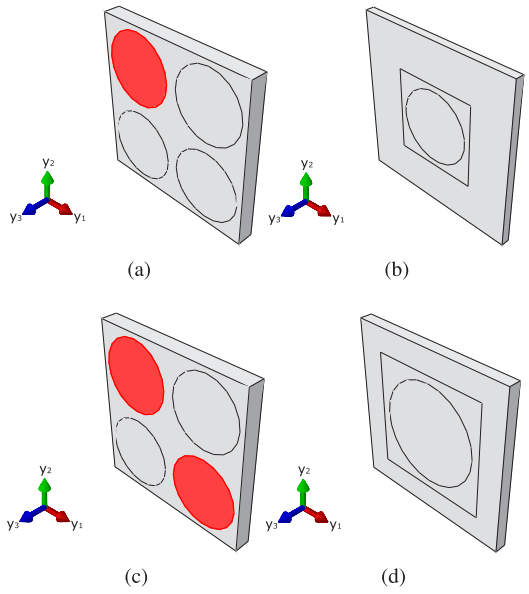

Fig. 10. Unit Cells used for the model with fiber degradation. (a) Standard four fiber UC with 1/4 of fibers damaged and (b) equivalent embedded model. (c) standard four fiber UC with 1/2 of fibers damaged and (d) equivalent embedded model.

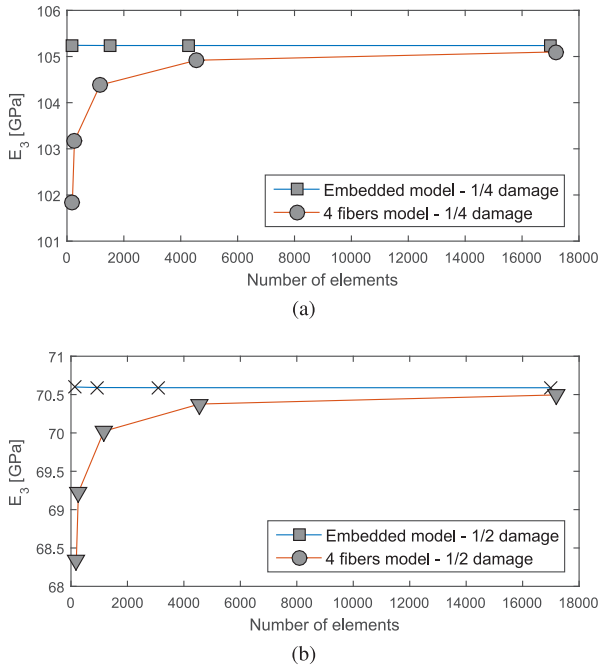

Fig. 11. Convergence analysis. Comparison between the standard four fiber UC and the embedded model. (a) 1/4 of fiber damaged. (b) 1/2 of fibers damaged.

In the next analyses, we want to demonstrate that the more complex the standard UC, the worse the mesh convergence rate is compared to the embedded model.

Therefore, we use standard Unit Cells comprised by 9 fibers and 16 fibers, and compare to their embedded counterpart. Fig. 12(a) and (c) show the standard UC models used to represent a domain with 2/9 and 7/9 of damaged fibers, respectively, and Fig. 12(b) and (d) show their embedded UC models counterparts. Fig. 13(a) and (b) show the convergence analysis for the cases with 2/9 of damaged fibers and 7/9 of damaged fibers, respectively.

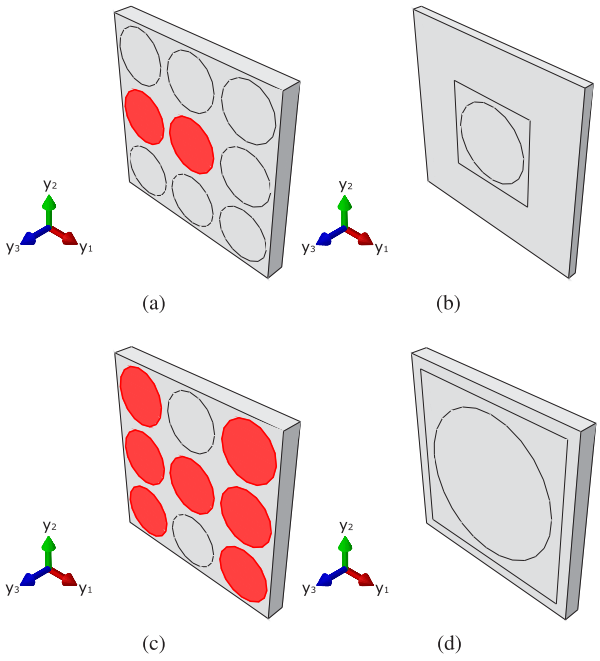

Fig. 12. Unit Cells used for the model with fiber degradation. (a) Standard nine fiber UC with 2/9 of fibers damaged and (b) equivalent embedded model. (c) standard nine fiber UC with 7/9 of fibers damaged and (d) equivalent embedded model.

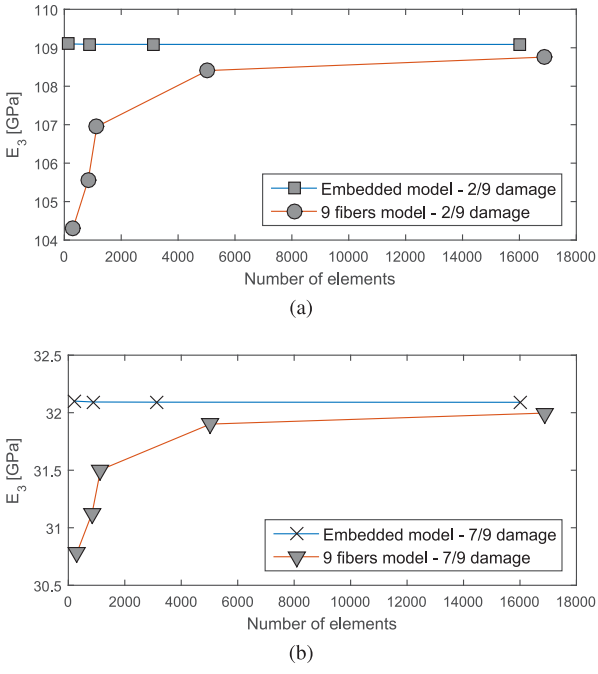

Fig. 13. Convergence analysis. Comparison between the standard nine fiber UC and the embedded model. (a) 2/9 of fiber damaged. (b) 7/9 of fibers damaged.

Figs. 14(a), 14 and 14(e) show the regular UC models used to represent a domain with 1/8, 1/2 and 7/8 of damaged fibers, respectively, and Fig. 14(b), (d) and (f) show their embedded UC models counterparts. Fig. 15(a), (b), and Fig. 15 show the convergence analysis for the cases with 1/8, 1/4, and 7/8 of damaged fibers, respectively.

For all cases, the standard RUC models used in simulation have to be modeled such that the volume fraction of the damaged fibers can be represented. As shown in Figs. 10, 12, and 14, depending on the fraction chosen for the analyses, the UC has to be modeled

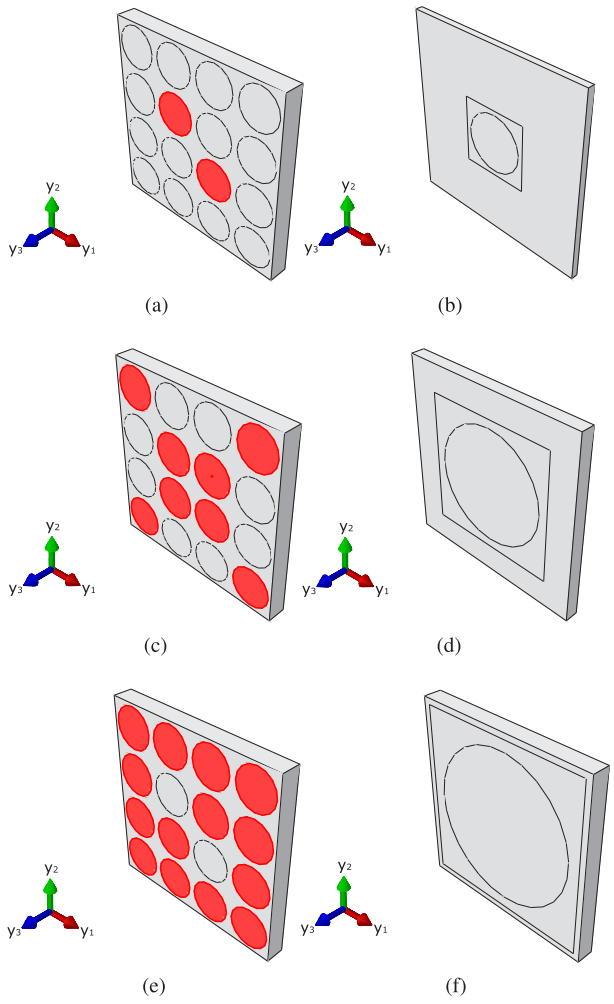

Fig. 14. Unit Cells used for the model with fiber degradation. (a) Standard sixteen fiber UC with 1/8 of fibers damaged and (b) equivalent embedded model. (c) standard sixteen fiber UC with 1/2 of fibers damaged and (d) equivalent embedded model. (e) standard sixteen fiber UC with 7/8 of fibers damaged and (d) equivalent embedded model.

with a specific number of fibers, which can increase significantly the complexity of the geometry. The multiscale embedded models, on the other hand, depict only a single damaged fiber, with an outer layer of homogenized intact material. In this case, the complexity of the geometry remains the same.

Despite representing the same portion of the media, with the same volume fraction of intact and damaged fibers, the standard, and the embedded UC models show a significant difference in the convergence of the finite element analyses, as shown in Figs. 11, 13 and 15. It can be seen that both approaches converge to the same value of the Elastic Modulus, however, the multiscale embedded models, for all cases analyzed, converge with fewer elements in comparison to the standard model. Thus, using embedded models, for this kind of analysis (effective Young's modulus in fiber direction), is a good alternative in the computational effort context.

As shown in the intact material analyses, the Elastic Modulus in the fiber direction is not affected by the fiber distribution. Thus, for the present case, the pattern of damage used does not influence the numerical value of the elastic modulus. However, as commented earlier, if the properties transversal to the fiber direction are considered, the fiber distribution, or distribution of the damage pattern, influences the mechanical properties.

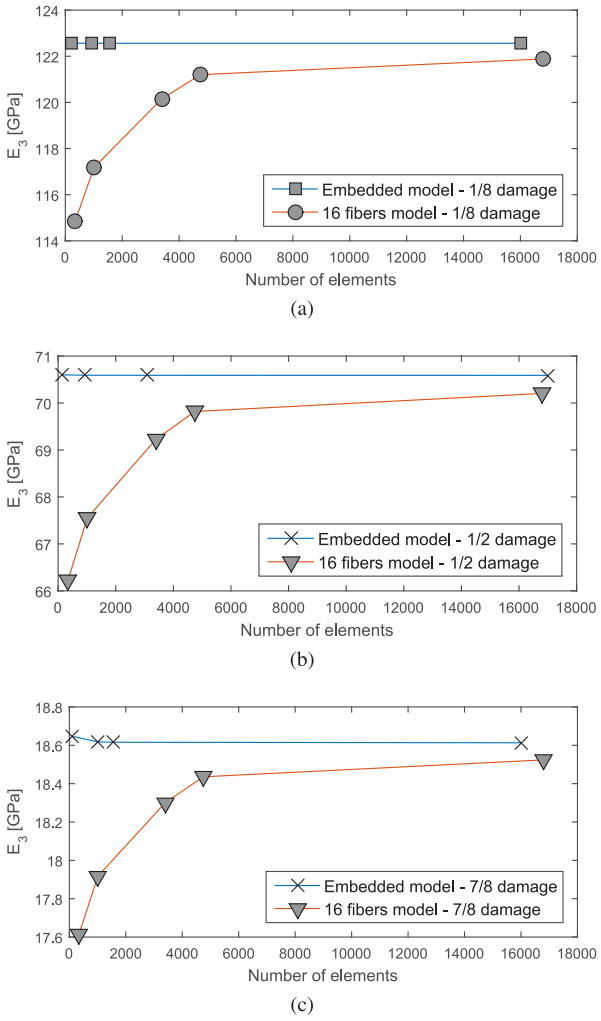

Fig. 15. Convergence analysis. Comparison between the standard sixteen fiber UC and the embedded model. (a) 1/8 of fiber damaged. (b) 1/2 of fibers damaged. (c) 7/8 of fibers damaged.

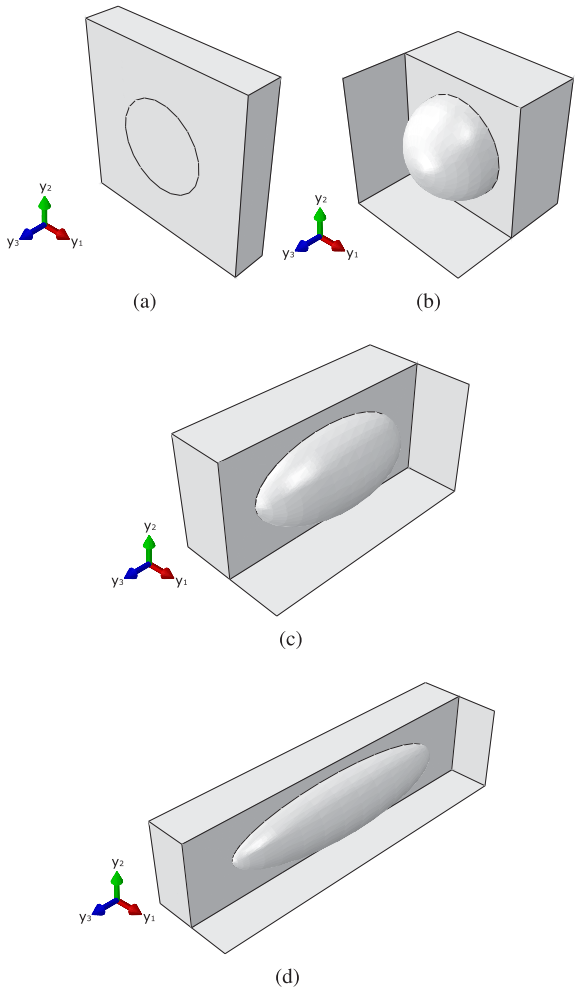

Fig. 16. Resin and void pockets. (a) cylindrical pocket; (b) spherical pocket; (c) ellipsoid pocket with $b = a/2$ and (d) ellipsoid pocket with $b = a/4$.

Those fiber damage patterns may appear in manufacturing processes during handling, although the percentage of broken fibers is typically low. This effect of broken fibers in the effective property in the fiber direction is negligible in real composites, however, as shown in [45], it has a significant effect on tensile strength. The authors show that the stress concentration on an intact fiber due to a neighboring broken fiber is high.

We chose the extreme values for fiber damage for comparing the multiscale embedded model and the standard Unit Cell model. A high percentage of damaged fibers might represent different stages of failure during a tensile test. Lastly, in the present study, only the fibers are considered to be damaged, which is an idealized model. More accurately, both fibers and matrix would fail.

4.3. Influence of resin and void pockets

In this section, the influence of resin and void pocket within an embedded UC on the effective properties of the media is investigated. Four different shapes of inclusions, representing both void and resin pockets, are considered. For resin pockets, it is used the material properties from Table 1. In all cases, the outer portion represents a homogenized intact material, whose properties were obtained in the previous sections. The inclusion shapes considered for the analyses are, cylindrical, spherical, an ellipsoid with $b = a/2$ and an ellipsoid with $b = a/4$, as shown in Fig. 16(a), (b), (c) and (d), respectively.

For all cases, volume fractions of the inclusions ranging from 0% to 40% are considered, and the effect on the effective elastic modulus in the fiber direction (y_3−direction) is investigated.

Fig. 17(a) shows the variation on the effective elastic modulus as a function of the resin pocket volume fraction, for all shapes of inclusions, while Fig. 17(b) shows the variation as a function of the void pocket volume fraction.

In both cases, the maximum difference of the effective elastic modulus is between the cylindrical and spherical inclusions. For a resin pocket with a volume fraction of 40%, the difference in the effective elastic modulus is 28%, and for a void pocket with the same volume fraction, the difference is 31%.

Fig. 18(a), (b), (c), and (d) show the comparison between the influence of resin and void pockets on the effective elastic modulus considering the cylindrical, spherical, ellipsoid with $b = a/2$, and ellipsoid with $b = a/4$ inclusions, respectively. In this comparison, a slight difference between the elastic modulus is noticed. For a volume fraction of resin and void pockets of 40%, the differences in the effective elastic modulus between both inclusion types are 1.5% for the cylindrical inclusions, 5.9% for the spherical inclusions, 4.42% for the ellipsoid inclusions with $b = a/2$, and 3.4% for the ellipsoid inclusions with $b = a/4$. This low difference in the effective elastic modulus is expected due to the order of magnitude of mechanical properties of the base materials.

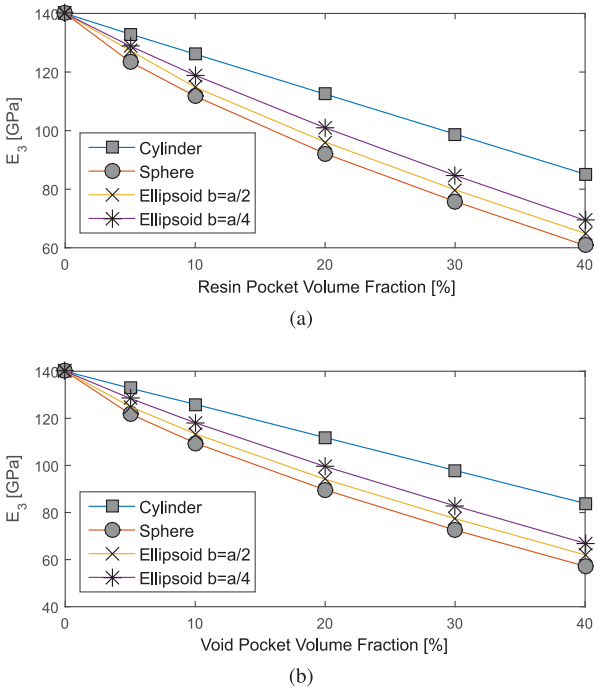

Fig. 17. Influence of (a) resin pockets, and (b) void pockets on the effective elastic modulus in the fiber direction considering four different inclusion shapes.

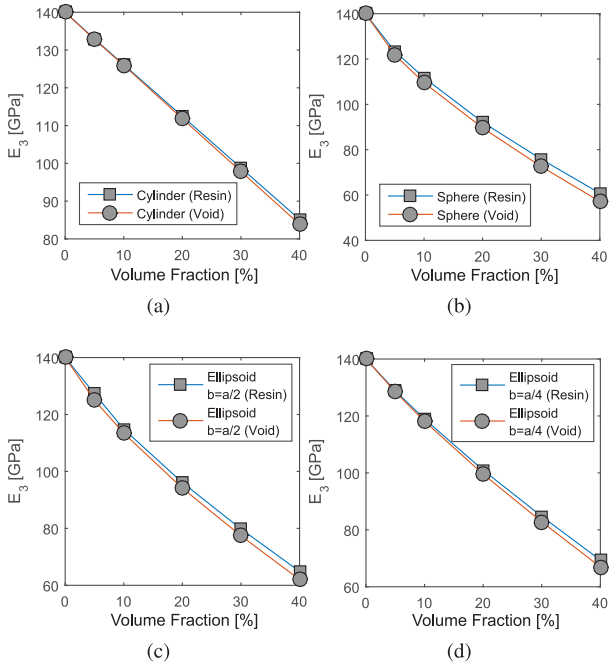

Fig. 18. Comparison between the influence of the resin and void pockets on the effective elastic modulus considering: (a) cylindrical inclusion; (b) spherical inclusion; (c) ellipsoid inclusion with $b = a/2$, and (d) ellipsoid inclusion with $b = a/4$.

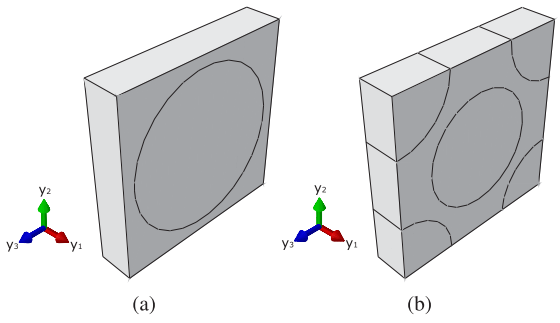

Fig. 19. Unit Cells used to obtain the complete fourth order elasticity tensor of the media: (a) UC 1 and (b) UC 2.

It is also observed that the mechanical properties of UC with fiber-aligned cylindrical inclusion are the least affected, while the mechanical properties of UC with spherical inclusion are the most affected. Unit Cells with elliptical inclusions have mechanical properties intermediately affected. Also, in limit cases, the ellipsoid approaches a sphere when $a \to b$, and a cylinder when $a \to \infty$, thus the intermediate effect on the mechanical properties is expected. When the cross-section of inclusions in the direction of the mechanical property of interest is considered, we observe that the area of the cylinder is the smallest among the chosen inclusions, while the area of the sphere is the largest. Thus, the behavior observed in Fig. 17 is coherent.

The presence of voids in the composites may be very high depending on the manufacturing process. The values accepted by the industry are nonetheless low. The results presented show that the mechanical properties are barely affected by the low volume fraction of voids. Moreover, the same reasoning is presented in [46], in which the authors show that the effect of a low volume fraction of voids in the elastic properties in the fiber direction is negligible. On the other hand, the presence of voids can have a significant effect on the properties transverse to the fibers.

Here, we demonstrate the use of the AHM-FEM method using an embedded Unit Cell and considering voids to obtain the mechanical properties in the fiber direction. The method may, however, be used to obtain all components of the elasticity tensor.

5. Determination of the complete fourth order elasticity tensor

In the previous cases, only the Elasticity Modulus in the fiber direction was obtained. The method, however, estimates the full fourth-order elasticity tensor of the heterogeneous media, as shown in Eq. (40). In this section, three different cases are considered to analyze the mechanical properties of a fiber-reinforced composite. The first analysis considers both the fiber and matrix as isotropic materials, and the second one considers the fiber as a transversely isotropic material. In both cases, two different standard Unit Cells, with different fiber distribution patterns, are used and the results are compared to literature data. The third analysis consists of an embedded model to estimate the effective properties of a metamaterial, in which a fiber-reinforced composite comprised of two different types of fibers, is considered.

5.1. Analyses considering the base materials as isotropic

Initially, both base materials are considered as isotropic, with mechanical properties given in Table 1 and fiber volume fraction $f_v = 0.6$. The Unit Cells considered for the analyses are shown in Fig. 19.

The results are compared to the literature data given in Table 3. All non-zero components of the tensor obtained by the AHM-FEM method are given in Table 4. As one can see, the results obtained by using both UC 1 and UC 2 approach the manufacturer data(Ref (iii)) for the elastic modulus in the fiber direction. The lack of a complete description of the material properties and the deviation among the literature results render the comparison of the other components hard to interpret. In addition, the comparison between the results obtained by both UC 1 and UC 2 models shows a good agreement.

Here, we assume both base materials as isotropic. This is a crude approximation since the fiber usually has a transversely isotropic behavior, which affects mainly the effective properties transverse to the

Table 3
Literature data for the effective mechanical properties of the material. Ref (i) [40]; Ref (ii) [43]; Ref (iii) [42]; Ref (iv) [44].

	Ref (i)	Ref (ii)	Ref (iii)	Ref (iv)
E_1 [GPa]	127	132	140	148
E_2 [GPa]	8.1	–	10.3	9.65
G_{12} [GPa]	–	4.39	6.5	4.55
G_{23} [GPa]	–	3.05	–	–
ν_{12}	0.34	0.327	0.25	0.3
ν_{23}	–	0.306	–	–

Table 4
Effective mechanical properties using the AHM-FEM approach with two different Unit Cells and considering the fiber as an isotropic material.

Material properties	UC 1	UC 2
E_1 [GPa]	139.60	139.63
E_2 [GPa]	15.92	10.03
G_{12} [GPa]	4.88	4.88
G_{23} [GPa]	3.30	3.22
ν_{12}	0.37	0.37
ν_{23}	0.24	0.26

Table 5
Literature data for the mechanical properties of the base materials (Fiber and Matrix) and effective properties of the composite ply [47].

Material properties	Fiber	Matrix	Ply
E_1 [GPa]	232.0	3.5	142.0
E_2 [GPa]	18.0	3.5	8.5
G_{12} [GPa]	8.7	1.25	3.7
G_{23} [GPa]	5.8	1.25	2.6
ν_{12}	0.2	0.35	0.25
ν_{23}	0.49	0.35	0.42

Table 6
Effective mechanical properties using the AHM-FEM approach with two different Unit Cells and considering the fiber as a transversely isotropic material.

Material properties	UC 1	UC 2
E_1 [GPa]	142.02	141.97
E_2 [GPa]	9.40	7.95
G_{12} [GPa]	3.60	3.59
G_{23} [GPa]	2.57	3.19
ν_{12}	0.25	0.25
ν_{23}	0.44	0.53

fiber direction. This might explain the deviation in some properties obtained by using the AHM-FEM approach.

Additionally, the complete description of the fiber properties by the manufacturers is rarely seen in the related data sheets. In addition, the complete description of the effective properties of a composite ply is also difficult to be found, mainly the out-of-plane properties.

5.2. Analyses considering the fiber as a transversely isotropic material

In a subsequent analysis, the fiber is considered transversely isotropic. The mechanical properties for the fiber and matrix, as well as the effective properties of the material, are given in Table 5 [47], and the fiber volume fraction is $f_v = 0.62$. The UC models shown in Fig. 19 are once more used for the analyses.

We can see that, with a complete description of the mechanical properties, the effective properties obtained by the AHM-FEM approach to the literature data. In addition, it is verified that the fiber distribution within the UC influences the effective properties of the media. This behavior is expected since the homogenized properties are dependent on the properties of the base materials, their volume fractions, and spatial distributions, as one can understand by analyzing Eqs. (34) and (39). Thus, one has to take into account the fiber distribution pattern on the media for modeling the UC, otherwise, some deviations in the results may be found.

Table 7
Mechanical properties of the SiC and Glass fibers [48].

Material properties	SiC	Glass Fiber
E [GPa]	450.0	73.1
ν	0.17	0.22

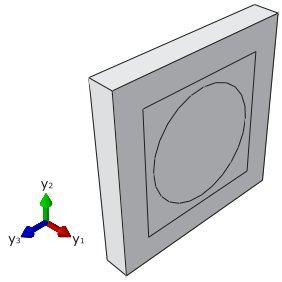

Fig. 20. Embedded UC model for the metamaterials. The outer portion represents a homogenized fiber reinforced composite, whilst the inner portion represents the matrix and different fibers (SiC and glass fiber) added to the metamaterial.

5.3. Applications to metamaterials

In this section, the AHM-FEM approach is applied to obtain the effective fourth-order elasticity tensor of metamaterials (mechanical properties). It is considered a unidirectional composite media comprised of a polymeric matrix reinforced by two different types of fibers.

An embedded UC, as shown in Fig. 20, is considered for all analyses. The outer portion of the UC is comprised of a homogenized material, whose properties were obtained in Table 6 using the Unit Cell designated of UC 1. The inner portion of the UC is comprised of the same matrix used in the previous case, but with a different type of fiber. We want to investigate the effect of adding a different material to the media on the homogenized mechanical properties. Thus, two different types of fiber are considered to be added to the media, silicon carbide fibers (SiC) and glass fibers, whose mechanical properties are given in Table 7, with a fiber volume fraction of 0.62. In addition, we also vary the volume fraction of the added material (matrix and new fibers) from 10% to 90% about the portion of the original material.

Fig. 21 shows the variation of the homogenized mechanical properties of the metamaterials as a function of the volume fraction of SiC and Glass Fibers obtained by the AHM-FEM approach.

Here, the AHM-FEM approach is used as a tool to assess the effective properties of a metamaterial, in which all independent elastic constants are obtained. The AHM, solved by the finite element method, can be used to obtain the effective properties of any kind of material, regardless of the properties of the base constituents, or their spatial distribution within the domain.

In addition, this approach can be combined with a least square method to obtain the spatial distribution and/or constituents of a UC to obtain a metamaterial with pre-defined mechanical properties.

6. Conclusions

In this work, an AHM-FEM approach is considered for simulating a virtual tensile test of a fiber-reinforced composite. The equilibrium relations are obtained by the Asymptotic Homogenization Method and solved within the Finite Element Package Abaqus™ to obtain the complete homogenized fourth-order elasticity tensor.

Initially, the elastic modulus in the fiber direction is investigated using several types of Unit Cells and convergence analyses are carried out to compare the computational efficiency of each case. All analyses converge to literature data. In addition, the effect of fiber failure and resin and void pockets within the domain is investigated. It is shown

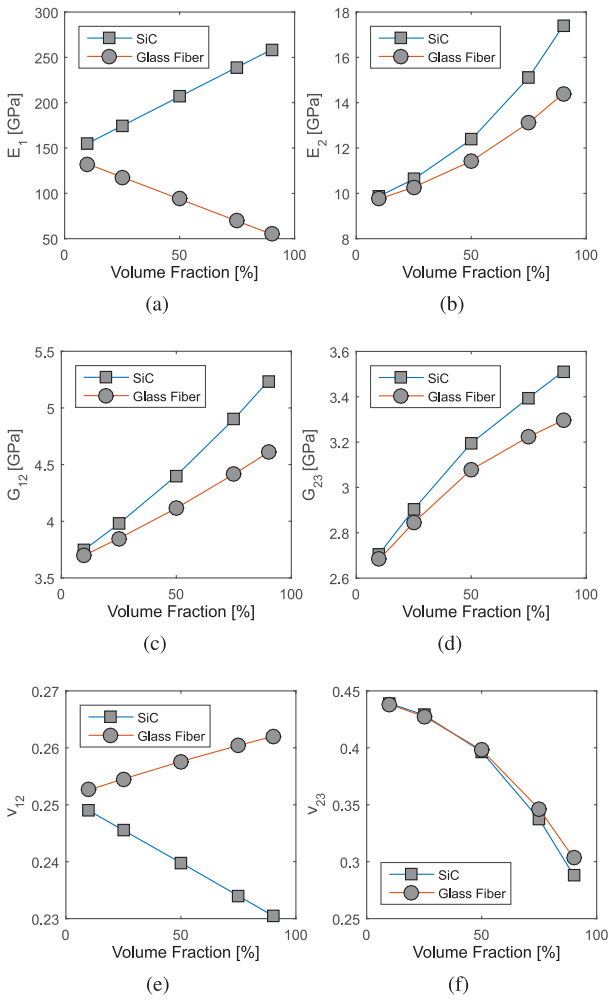

Fig. 21. Variation of the mechanical properties of the metamaterials as a function of the volume fraction of the added materials: (a) E_1; (b) E_2; (c) G_{12}; (d) G_{23}; (e) ν_{12}; (f) ν_{23}.

that multiscale embedded UC models are a good alternative to standard UC models when computational efficiency is considered.

In further analyses, the complete homogenized fourth-order elasticity tensor of the media (mechanical properties) is investigated by considering the fibers as isotropic and as transversely isotropic. It is shown that an isotropic fiber is not a good approximation to estimate the effective properties of the media. On the other hand, for transversely isotropic fibers, the homogenized properties of the media approach literature data.

The approach is extended to obtain the mechanical properties of metamaterials, in which a composite reinforced by two types of fibers is considered. The AHM-FEM approach, as implemented in this work, may be used to assess the effective properties of any kind of metamaterial, regardless of the base materials, and their shapes, comprising the media.

The analyses show how robust the AHM-FEM approach is to assess the effective properties of a fiber-reinforced composite and how it may be used to improve the computational efficiency of the numerical simulations.

Declaration of competing interest

The authors declare that they have no known competing financial interests or personal relationships that could have appeared to influence the work reported in this paper.

Acknowledgments

Volnei Tita acknowledges CNPq, Brazil (process No. 310656/2018-4),
CAPES-FCT, Brazil (No. AUXPE 88881.467834/2019-01 - Finance Code 001), and FAPESP-FAPERGS, Brazil (process number: 2019/15179-2 and 19/2551). The author Humberto Brito-Santana would like to thank LPR19-09 (Proyecto interno de la Universidad Tecnológica Metropolitana, Brazil) for financial support.

References

[1] M. Romanowicz, Prediction of elastic moduli of angle-ply laminates from various rhombohedral unit cells, Mech. Adv. Mater. Struct. 26 (4) (2019) 307–313.
[2] R.M. Jones, Mechanics of Composite Materials, CRC Press, 2018.
[3] F. Marinelli, A.P. Van den Eijnden, Y. Sieffert, R. Chambon, F. Collin, Modeling of granular solids with computational homogenization: Comparison with Biot' s theory, Finite Elem. Anal. Des. 119 (2016) 45–62.
[4] E. Sanchez-Palencia, Comportements local et macroscopique d'un type de milieux physiques hétérogènes, Internat. J. Engrg. Sci. 12 (4) (1974) 331–351.
[5] E.W. Larsen, Neutron transport and diffusion in inhomogeneous media. I, J. Math. Phys. 16 (7) (1975) 1421–1427.
[6] J.B. Keller, Effective behavior of heterogeneous media, in: Statistical Mechanics and Statistical Methods in Theory and Application, Springer US, 1977, pp. 631–644.
[7] D. Cioranescu, J.S.J. Paulin, Homogenization in open sets with holes, J. Math. Anal. Appl. 71 (2) (1979) 590–607.
[8] E. Sánchez-Palencia, Non-homogeneous media and vibration theory, Lect. Notes Phys. 127 (1980).
[9] F. Lene, D. Leguillon, Homogenized constitutive law for a partially cohesive composite material, Int. J. Solids Struct. 18 (5) (1982) 443–458.
[10] A. Oleinik, G.P. Panasenko, G.A. Yosifian, Homogenization and asymptotic expansions for solutions of the elasticity system with rapidly oscillating periodic coefficients, Appl. Anal. 15 (1–4) (1983) 15–32.
[11] E. Sanchez-Palencia, Homogenization in mechanics. A survey of solved and open problems, Rend. Semin. Mat. Univ. Politec. Torino 44 (1) (1986) 1–45.
[12] N. Panasenko, N.S. Bakhvalov, Homogenization: averaging processes in periodic media: mathematical problems in the mechanics of composite materials, Math. Appl. 36 (1989).
[13] J. Guedes, N. Kikuchi, Preprocessing and postprocessing for materials based on the homogenization method with adaptive finite element methods, Comput. Methods Appl. Mech. Engrg. 83 (2) (1990) 143–198.
[14] B. Hassani, E. Hinton, A review of homogenization and topology optimization I—homogenization theory for media with periodic structure, Comput. Struct. 69 (6) (1998) 707–717.
[15] B. Hassani, E. Hinton, A review of homogenization and topology opimization II—analytical and numerical solution of homogenization equations, Comput. Struct. 69 (6) (1998) 719–738.
[16] R.Q. de Macedo, R.T.L. Ferreira, J.M. Guedes, M.V. Donadon, Intraply failure criterion for unidirectional fiber reinforced composites by means of asymptotic homogenization, Compos. Struct. 159 (2017) 335–349.
[17] J.A. Otero, R. Rodríguez-Ramos, J. Bravo-Castillero, R. Guinovart-Díaz, F.J. Sabina, G. Monsivais, Semi-analytical method for computing effective properties in elastic composite under imperfect contact, International Journal of Solids and Structures 50 (3-4) (2013) 609–622.
[18] R.Q. de Macedo, R.T.L. Ferreira, M.V. Donadon, J.M. Guedes, Elastic properties of unidirectional fiber-reinforced composites using asymptotic homogenization techniques, J. Braz. Soc. Mech. Sci. Eng. 40 (5) (2018) 1–11.
[19] F.J. Sabina, Y. Espinosa-Almeyda, R. Guinovart-Díaz, R. Rodríguez-Ramos, H. Camacho-Montes, Effective complex properties for three-phase elastic fiber-reinforced composites with different unit cells, Technologies 9 (1) (2021) 12.
[20] H. Camacho Montes, F.J. Sabina, Y. Espinosa Almeyda, R. Guinovart Díaz, R. Rodríguez Ramos, Effective Complex Properties for Three-Phase Elastic Fiber-Reinforced Composites with Different Unit Cells, Instituto de Ingeniería Y Tecnología, 2021.
[21] H. Brito-Santana, R. de Medeiros, A.J.M. Ferreira, R. Rodríguez-Ramos, V. Tita, Effective elastic properties of layered composites considering non-uniform imperfect adhesion, Appl. Math. Model. 59 (2018) 183–204.
[22] H. Brito-Santana, J.L.M. Thiesen, R. de Medeiros, A.J.M. Ferreira, R. Rodríguez-Ramos, V. Tita, Multiscale analysis for predicting the constitutive tensor effective coefficients of layered composites with micro and macro failures, Appl. Math. Model. 75 (2019) 250–266.
[23] B.G. Christoff, H. Brito-Santana, V. Tita, Analysis of unbalanced composites with imperfect interphase: effective properties via asymptotic homogenization method., Proc. Inst. Mech. Eng. L - J. Mater.-Des. Appl. (2021).

[24] A. Ramírez-Torres, R. Penta, R. Rodríguez-Ramos, A. Grillo, L. Preziosi, J. Merodio, R. Guinovart-Díaz, J. Bravo-Castillero, Homogenized out-of-plane shear response of three-scale fiber-reinforced composites, Comput. Vis. Sci. 20 (3) (2019) 85–93.
[25] A. Ramírez-Torres, R. Penta, R. Rodríguez-Ramos, A. Grillo, Effective properties of hierarchical fiber-reinforced composites via a three-scale asymptotic homogenization approach, Math. Mech. Solids 24 (11) (2019) 3554–3574.
[26] R. Rodríguez-Ramos, A. Ramírez-Torres, J. Bravo-Castillero, R. Guinovart-Díaz, D. Guinovart-Sanjuán, O.L. Cruz-González, F.J. Sabina, J. Merodio, R. Penta, Multiscale homogenization for linear mechanics, in: Constitutive Modelling of Solid Continua, Springer, 2020, pp. 357–389.
[27] D. Garoz, F. Gilabert, R. Sevenois, S. Spronk, W. Van Paepegem, Consistent application of periodic boundary conditions in implicit and explicit finite element simulations of damage in composites, Composites B 168 (2019) 254–266.
[28] M. Ameen, R.H.J. Peerlings, M.G.D. Geers, Higher-order asymptotic homogenization of periodic linear elastic composite materials at low scale separation, in: 24th International Congress of Theoretical and Applied Mechanics (ICTAM 2016), IUTAM, 2017, pp. 2544–2545.
[29] S.J. Hollister, N. Kikuchi, A comparison of homogenization and standard mechanics analyses for periodic porous composites, Comput. Mech. 10 (2) (1992) 73–95.
[30] R. Rodríguez-Ramos, R. de Medeiros, R. Guinovart-Díaz, J. Bravo-Castillero, J.A. Otero, V. Tita, Different approaches for calculating the effective elastic properties in composite materials under imperfect contact adherence, Compos. Struct. 99 (2013) 264–275.
[31] M. Tapia, Y. Espinosa-Almeyda, R. Rodríguez-Ramos, J.A. Otero, Computation of effective elastic properties using a three-dimensional semi-analytical approach for transversely isotropic nanocomposites, Appl. Sci. 11 (4) (2021) 1867.
[32] T.A. Dutra, R.T.L. Ferreira, H.B. Resende, A. Guimarães, J.M. Guedes, A complete implementation methodology for asymptotic homogenization using a finite element commercial software: preprocessing and postprocessing, Compos. Struct. 245 (2020) 112305.
[33] B.G. Christoff, H. Brito-Santana, R. Talreja, V. Tita, Development of an ABAQUS^{TM} plug-in to evaluate the fourth-order elasticity tensor of a periodic material via homogenization by the asymptotic expansion method, Finite Elem. Anal. Des. 181 (2020) 103482.
[34] S. Yang, T. Gao, C. Shen, Simple implementation of asymptotic homogenization method for periodic composite materials, in: Materials Science Forum, Vol. 1015, Trans Tech Publ, 2020, pp. 57–63.
[35] B.L. Silva, B.G. Christoff, C.M. Lepienski, E.L. Cardoso, L.A. Coelho, D. Becker, Role of cured epoxy and block copolymer addition in mechanical and thermal properties of polyethylene, Mater. Res. 20 (2017) 1221–1229.
[36] H. Brito-Santana, B.G. Christoff, A.J.M. Ferreira, F. Lebon, R. Rodríguez-Ramos, V. Tita, Delamination influence on elastic properties of laminated composites, Acta Mech. 230 (3) (2019) 821–837.
[37] S.J. Hollister, N. Kikuchi, Homogenization theory and digital imaging: A basis for studying the mechanics and design principles of bone tissue, 43, (7), 1994, 586–596, http://dx.doi.org/10.1002/bit.260430708.
[38] Z. Fang, W. Sun, J.T. Tzeng, Asymptotic homogenization and numerical implementation to predict the effective mechanical properties for electromagnetic composite conductor, J. Compos. Mater. 38 (16) (2004) 1371–1385.
[39] O.C. Zienkiewicz, R.L. Taylor, R.L. Taylor, R.L. Taylor, The Finite Element Method: Solid Mechanics, Vol. 2, Butterworth-heinemann, 2000.
[40] V. Tita, J. De Carvalho, D. Vandepitte, Failure analysis of low velocity impact on thin composite laminates: Experimental and numerical approaches, Compos. Struct. 83 (4) (2008) 413–428.
[41] Hexcel® Corporation, Hextow® carbon fiber, 2020.
[42] Hexcel® Corporation, Hexply® M10r 120° c curing epoxy matrix, 2015.
[43] D.B. Miracle, S.L. Donaldson, S.D. Henry, C. Moosbrugger, G.J. Anton, B.R. Sanders, N. Hrivnak, C. Terman, J. Kinson, K. Muldoon, et al., ASM Handbook, Vol. 21, 2001.
[44] S. Tsai, Composites Design, United States Air Force Materials Laboratory, Think Composites, Dayton, 1986.
[45] L. Zhuang, R. Talreja, J. Varna, Tensile failure of unidirectional composites from a local fracture plane, Compos. Sci. Technol. 133 (2016) 119–127.
[46] H. Huang, R. Talreja, Effects of void geometry on elastic properties of unidirectional fiber reinforced composites, Compos. Sci. Technol. 65 (13) (2005) 1964–1981.
[47] L. Wang, C. Zheng, S. Wei, Z. Wei, Micromechanics-based progressive failure analysis of carbon fiber/epoxy composite vessel under combined internal pressure and thermomechanical loading, Composites B 89 (2016) 77–84.
[48] H. Brito-Santana, R. de Medeiros, R. Rodriguez-Ramos, V. Tita, Different interface models for calculating the effective properties in piezoelectric composite materials with imperfect fiber–matrix adhesion, Compos. Struct. 151 (2016) 70–80.